Rhodopsin Dynamics

DOI: 10.1002/anie.201309581

Characterization of the Simultaneous Decay Kinetics of Metarhodopsin States II and III in Rhodopsin by Solution-State NMR Spectroscopy**

*Jochen Stehle, Robert Silvers, Karla Werner, Deep Chatterjee, Santosh Gande, Frank Scholz, Arpana Dutta, Josef Wachtveitl, Judith Klein-Seetharaman, and Harald Schwalbe**

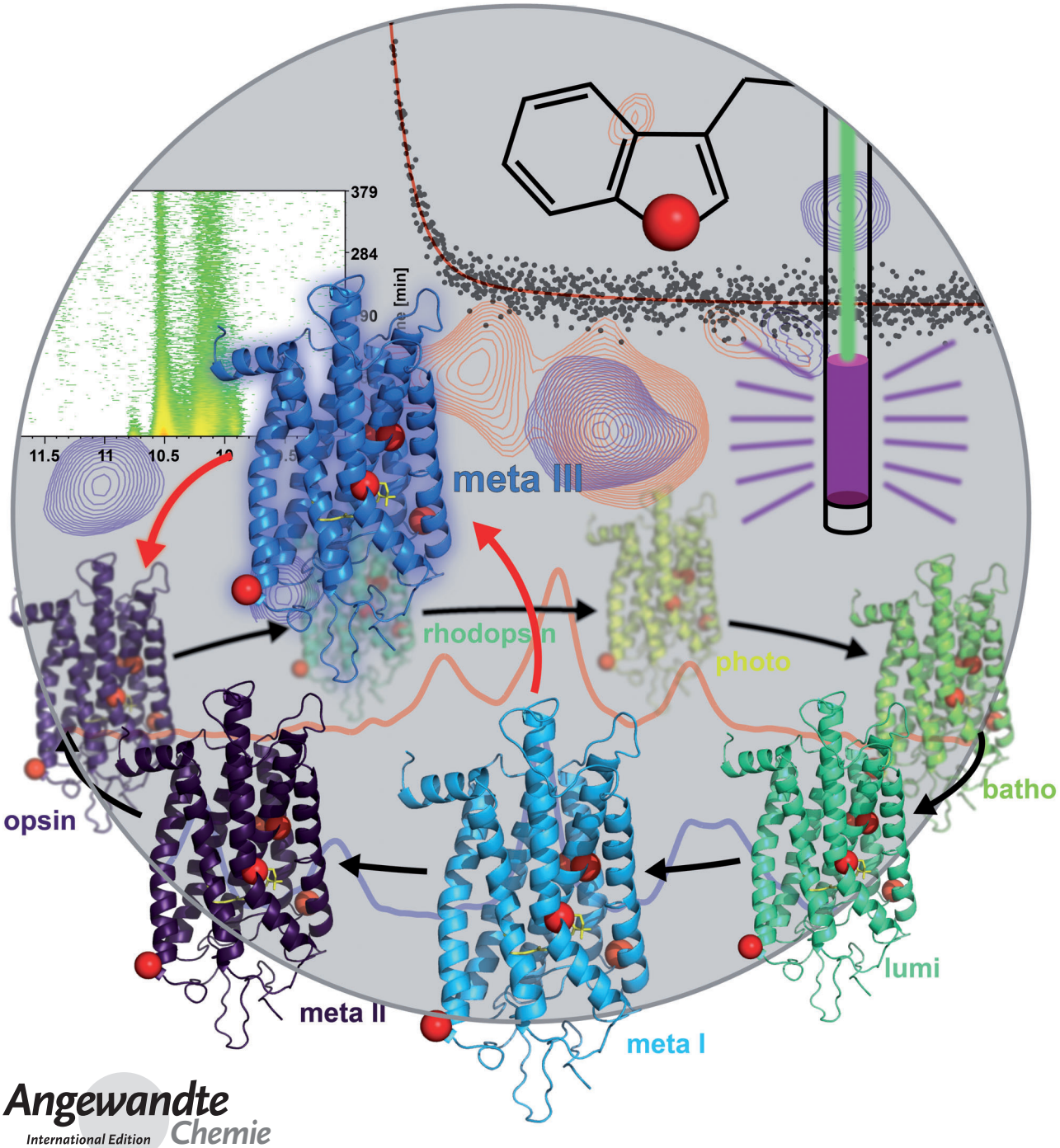

Abstract: *The mammalian visual dim-light photoreceptor rhodopsin is considered a prototype G protein-coupled receptor. Here, we characterize the kinetics of its light-activation process. Milligram quantities of α,ε-^{15}N-labeled tryptophan rhodopsin were produced in stably transfected HEK293 cells. Assignment of the chemical shifts of the indole signals was achieved by generating the single-point-tryptophan to phenylalanine mutants, and the kinetics of each of the five tryptophan residues were recorded. We find kinetic partitioning in rhodopsin decay, including three half-lives, that reveal two parallel processes subsequent to rhodopsin activation that are related to the photocycle. The meta II and meta III states emerge in parallel with a relative ratio of about 3:1. Transient formation of the meta III state was confirmed by flash photolysis experiments. From analysis of the site-resolved kinetic data we propose the involvement of the E_2-loop in the formation of the meta III state.*

One of the most thoroughly studied G protein-coupled receptors (GPCRs) is the mammalian visual dim-light photoreceptor rhodopsin. The apo-protein, referred to as opsin, is covalently attached to the chromophore 11-*cis*-retinal through formation of a Schiff base. Photon absorption results in the isomerization of retinal to the *all-trans* configuration and conformational changes in the protein through a complex photocycle in which several intermediate states are transiently populated. These states differ significantly in their light absorption, structure, and dynamics and have been intensively studied.[2] The absorption maximum of the rhodopsin-bound chromophore shifts from 380 to 570 nm during the photocycle (Figure 1).[2a,3] Crystal structures are available for four of the kinetically identified intermediates, while some intermediates can be captured at low temperatures and in time-resolved experiments.[1,4] The metarhodopsin I (meta I) state is the first state, where significant helix rearrangements occur.[5] The photocycle can progress via two different intermediates, metarhodopsin II (meta II, $\lambda = 380$ nm) or metarhodopsin III (meta III, $\lambda = 465$ nm).[6] After reaching the meta II/meta III states, the photocycle slows down significantly to a regime on the minute timescale.[7] The conversion of meta I into meta II is the major pathway and constitutes the key event in the photocycle. The absorption maximum (λ_{max}) is shifted by about 100 nm ($\lambda = 478$ nm to $\lambda = 380$ nm). The meta I state is inactive, and it is the meta II state[2b] that transmits the light signal to the visual G protein. The lifetime of the interaction of the G protein with rhodopsin has been reported to last approximately 100 ms and is interrupted by rhodopsin kinase and arrestin.[8] The active meta II state has a life-time of several minutes and decays to opsin and retinal.[7] The formation of meta III from meta I has been reported to represent a minor pathway. Since the meta III state is not active in signaling,[9] it is thought to represent a storage state of the light-receptor rhodopsin that is important for regeneration of the photoreceptor. This storage of activated rhodopsin could also play a significant role in the light adaptation process, since an already saturated light receptor cannot be excited further.[6a]

The changes in the photophysics of retinal are linked to structural and dynamic changes in the protein. A number of crystal structures have been solved (see Figure 1[2a,c-f,10,11]). We linked those crystal states by molecular morphing (see Movie S1 in the Supporting Information). From inspection of the movie, it is apparent that the most important conformational change during the photocycle is a tilt movement of helix 6 induced by disruption of the interaction network at the cytoplasmic ends of helices 3 and 6, commonly referred to as the "ionic lock" and involving the highly conserved D/ERY motif in helix 3 (see Movie S1 at times (min:s) 0:09–0:22). In a concerted process, a second set of interactions involving the cytoplasmic end of helix 7, especially F313, and helix 8, are rearranged, in particular of Y306 which is part of the conserved NPXXY motif (see Movie S1 at times 0:24–0:37).[12]

While these crystal structures provide snapshot views of major intermediates in the photocycle, understanding the dynamics of the transitions between conformations in solution and especially of the competing decay paths from meta I to meta II or meta III requires studies under more physiologically relevant conditions. NMR spectroscopy in solution is ideally suited to address these questions.[13,14] The kinetics of the photocycle have previously been monitored by 1D ^{19}F NMR spectroscopy, and ^{19}F chemical shifts could be differentiated between dark and meta II states as well as during the decay of meta II.[13a]

To gain insight into the dynamic equilibrium of structures formed upon activation with light, we carried out time-resolved solution NMR experiments on α,ε-^{15}N-tryptophan-labeled rhodopsin, complemented by optical data from flash photolysis experiments. We unambiguously assigned all five tryptophan resonances in dark-state rhodopsin, thus allowing us to measure the kinetics for the five tryptophan reporter signals upon activation with light. Analysis of the kinetic data reveals differences in the decay kinetics of the five signals and a significant kinetic partitioning of the decay of light-activated rhodopsin, thereby suggesting that both meta II and meta III states are populated under our experimental

[*] Dr. J. Stehle, Dr. R. Silvers, Dr. K. Werner, D. Chatterjee, Dr. S. Gande, Prof. Dr. H. Schwalbe
Institute for Organic Chemistry and Chemical Biology
Center of Biomolecular Magnetic Resonance
Johann Wolfgang Goethe-University Frankfurt
Max-von-Laue-Strasse 7, 60438 Frankfurt am Main (Germany)
E-mail: schwalbe@nmr.uni-frankfurt.de
F. Scholz, Prof. Dr. J. Wachtveitl
Institute of Physical and Theoretical Chemistry
Goethe University Frankfurt
60438 Frankfurt (Germany)
A. Dutta, Prof. Dr. J. Klein-Seetharaman
Division of Metabolic and Vascular Health, Medical School
University of Warwick, Coventry CV4 7AL (UK)

[**] The work was supported by the DFG grant SFB807. H.S. and J.W. are members of the DFG-funded cluster of excellence: macromolecular complexes. BMRZ is supported by the state of Hesse. J.K.-S. is supported by NSF grant 1144281.

Supporting information for this article (Experimental details)[14b,16,24] is available on the WWW under http://dx.doi.org/10.1002/anie.201309581.

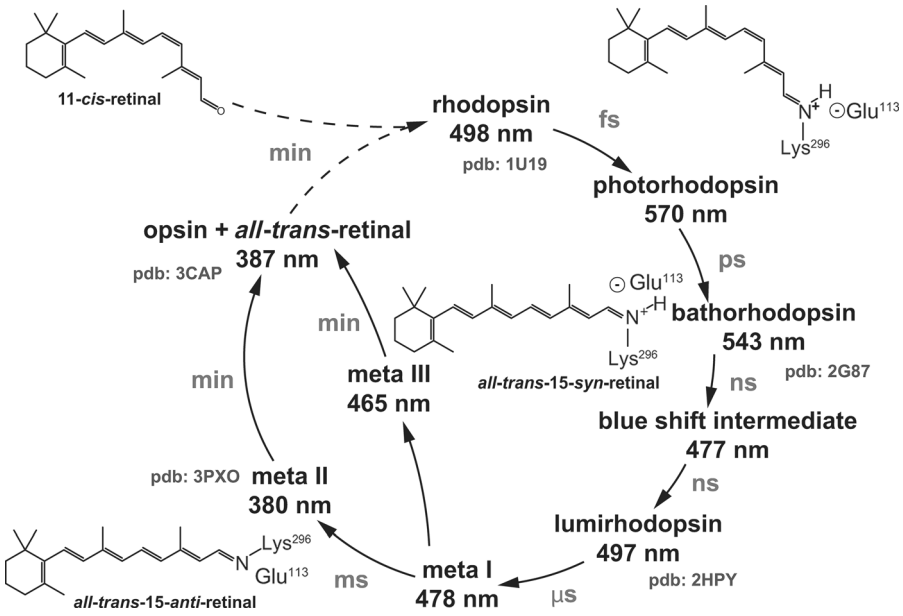

Figure 1. The photocycle of bovine rhodopsin, adapted from Ref. [1]. The photocycle involves several intermediates defined by their absorption characteristics. The first detectable intermediate after illumination is photorhodopsin, and subsequent intermediates emerge through thermal relaxation: The conversion of meta I into meta II is a key event within the rhodopsin photocycle, and constitutes the transition from the inactive state to the signal-transducing state of rhodopsin. In the meta II state, the Schiff base is deprotonated and the retinal is present in its *all-trans*-15-*anti* configuration. During the decay of meta II, retinal dissociates from rhodopsin, thereby resulting in free retinal and opsin. Meta III is an alternative intermediate on a second meta I decay pathway.

conditions, a proposal fully supported by the reported flash photolysis experiments. ^{15}N-Filtered NMR spectra of α,ε-^{15}N-tryptophan-labeled rhodopsin show five proton resonances in the indole region which correspond to the five tryptophan moieties present in bovine rhodopsin (Figure 2, Figure S1). The ^{1}H NMR spectra of unlabeled rhodopsin show several additional signals stemming from backbone amide protons in this region (see Figure S2). Previous attempts to assign the NMR chemical shifts of the tryptophan indole resonances failed because of an insufficient signal-to-noise ratio in the correlation experiments.[14b,15] Therefore, we assigned the five tryptophan indole resonances by utilizing single-point tryptophan to phenylalanine mutants. Each of these rhodopsin mutants then shows only four of the five NMR resonances in the indole region (Figure 2B). Rhodopsin was illuminated in situ in the NMR spectrometer by using an argon ion laser as the light source that was coupled to the NMR measuring tube through fiberglass optics.[16] By using fast NMR-acquisition schemes optimized for spectral resolution through a highly narrow spectral width in the indirect dimension it was possible to record a series of heteronuclear 2D NMR spectra of α,ε-^{15}N-tryptophan-labeled rhodopsin with a temporal resolution of one minute. The first 2D ^{1}H,^{15}N-SOFAST HMQC spectrum after the illumination pulse is shown in Figure 3 (see Figure S5 in the Supporting Information for the series of 2D ^{1}H,^{15}N-SOFAST HMQC spectra recorded subsequently in one minute intervals). As a result of previous kinetic analyses revealing that the early intermediates have very short lifetimes, we can assign the first spectrum after illumination to a mixture of states mainly composed of meta II and meta III states. During the meta II/III decay, the Schiff base is cleaved and retinal is irreversibly (in vitro) released from rhodopsin. The dissociation of retinal from opsin initiates aggregation, thus resulting in a decrease in the signal intensities over several hours.

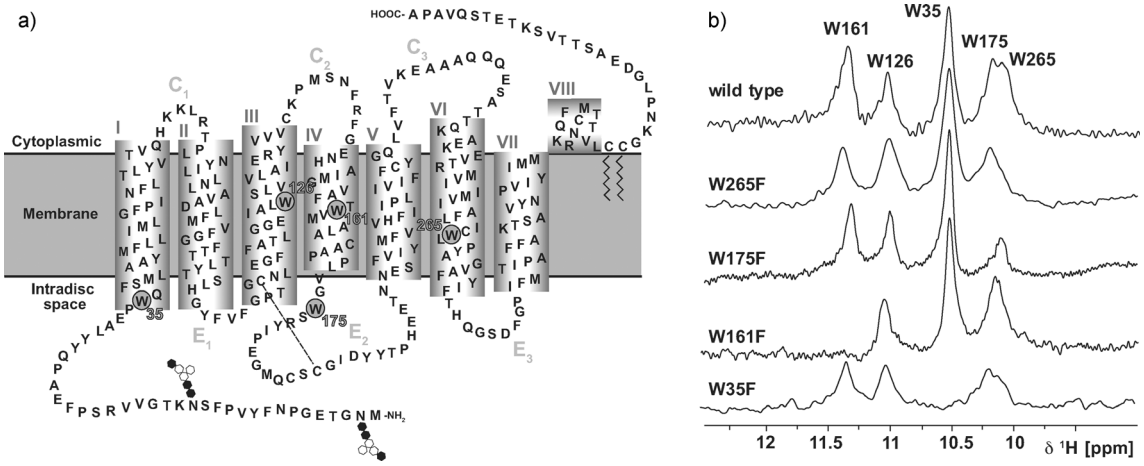

Figure 2. a) Secondary structure of bovine rhodopsin. The five tryptophan residues (W35, W126, W161, W175, and W265) used as reporter groups in the NMR experiments are indicated. b) Overlay of the indole region of 1D ^{1}H NMR spectra of α,ε-^{15}N-tryptophan-labeled dark-state rhodopsin and the tryptophan to phenylalanine mutants: W35F, W161F, W175F, and W265F.

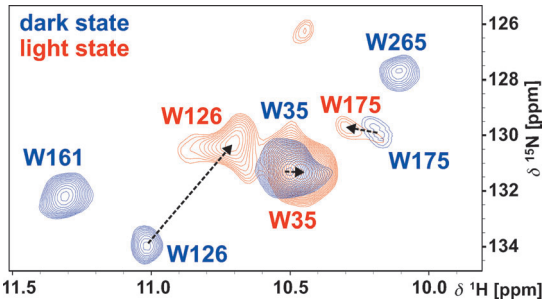

Figure 3. SOFAST HMQC spectra of the indole region of dark-state rhodopsin (blue) and light-activated-state rhodopsin (red). NMR chemical shift assignments in the dark state were transferred from 1D dimensional NMR spectra. Spectra were recorded at 800 MHz proton frequency at $T = 298$ K.

NMR chemical shifts are highly sensitive to the chemical environment, and the resonance pattern changes significantly after illumination. Only the resonances for W35 and W175 show relatively small changes in their chemical shifts upon activation with light (Figure 4a). In contrast, the resonances corresponding to W161 and W265 in the dark state are no longer observable in the light-activated state of ^{15}N-labeled rhodopsin immediately after illumination. The resonances corresponding to W265 recover and rise to a maximum after approximately 15 minutes, while the resonance corresponding to W161 can be detected only in unlabeled rhodopsin at higher concentrations (see Figure S2). The chemical shift of the resonance corresponding to W126 undergoes a large perturbation. Kinetic deconvolution of the decay data after light activation reveals three time regimes (Figure 4). The first half-life (t_1) is in the range of four to five minutes, the second process has a half-life (t_2) in the range of 21 to 25 minutes, and the third process has a half-life (t_3) on the order of two to three hours. The half-life t_3 has large error bars and can be detected only through changes in the amplitude of signals corresponding to W175 and W265. Half-life t_3 most likely corresponds to an aggregation process initiated after the dissociation of retinal from opsin. This conclusion is also supported by the observation that the kinetics are irreversible and the end state is invisible to solution-state NMR spectroscopy. Aggregation of rhodopsin is also confirmed by precipitation in the NMR tube after several hours. We thus disregard this third process, since the half-life of 2–3 h exceeds the time range of the physiological activity of rhodopsin. Kinetic analysis could also be conducted with two mutants of sufficient concentration (see Figure S4). The process corresponding to the time constant t_1 shows an amplitude of $73 \pm 8\,\%$, whereas the slow process shows an amplitude of $26 \pm 7\,\%$.

To confirm that the meta III state indeed forms under our NMR conditions (solubilized protein in *n*-dodecyl-β-D-maltoside (DDM) micelles), we performed flash photolysis experiments under identical conditions. The meta III absorption maximum ($\lambda = 465$ nm) differs considerably from the absorption maximum of the meta II state ($\lambda = 380$ nm) and is close to the absorption maximum of the dark state ($\lambda = 500$ nm). Continuous illumination led to a depletion of the absorption maximum of the dark state and a rise of an absorption around 380 nm (Figure 5a), which corresponds to the meta II state. Time-resolved absorption changes at 500 nm and 380 nm after photoexcitation revealed an interconversion of both species

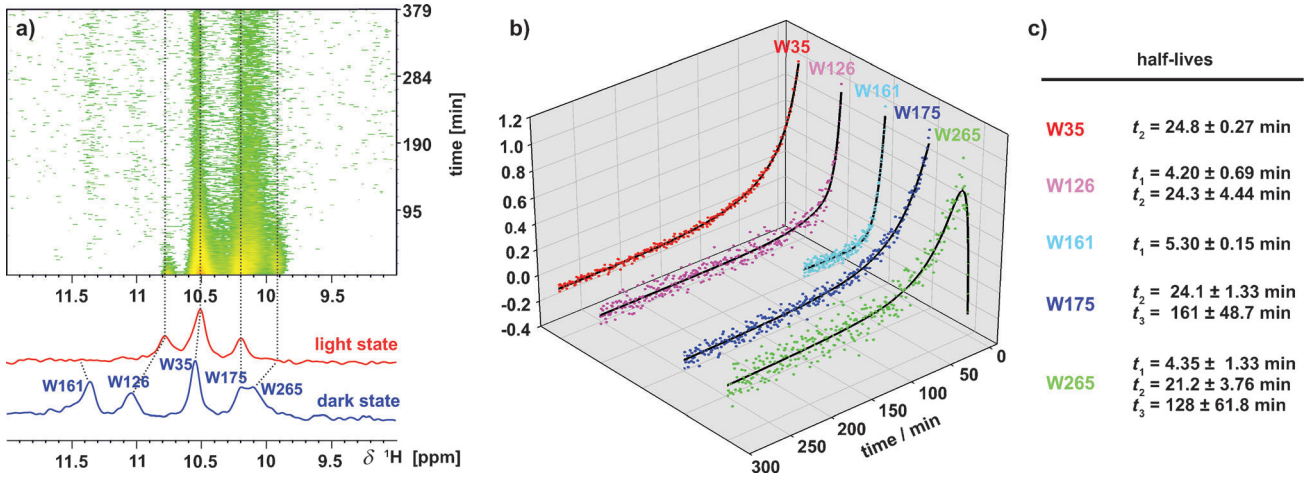

Figure 4. a) A series of 1D ^{1}H NMR spectra of α,ε-^{15}N-tryptophan-labeled rhodopsin recorded at different time intervals after illumination. The indole region of the spectrum is shown. The five resonances visible in the dark state correspond to the five tryptophan residues present in rhodopsin. Subsequent to illumination, 1D ^{1}H spectra were recorded with a temporal resolution of one minute. The blue spectrum corresponds to the indole region of dark-state rhodopsin and the red spectrum corresponds to the light-activated state of rhodopsin. The dashed lines connect the corresponding resonances before and after illumination. For W161, the dashed connection was transferred from 1D ^{1}H NMR spectrum of the unlabeled rhodopsin sample (see Figure S2). b) Extracted signal intensities from the series of 1D ^{1}H NMR spectra of α,ε-^{15}N-tryptophan-labeled rhodopsin. The signal intensities were normalized and plotted as a function of time. Different fitting routines have been applied to accommodate for the individual graph properties of each signal row. A mono-exponential fitting routine was applied for the signal intensities of W35 and W161, a biexponential fitting routine was applied for the signal intensities of W126 and W175, and a triexponential fitting routine was applied for the signal intensities of W265. c) Half-lives for each tryptophan indole ring were extracted by exponential fit (Figure S3).

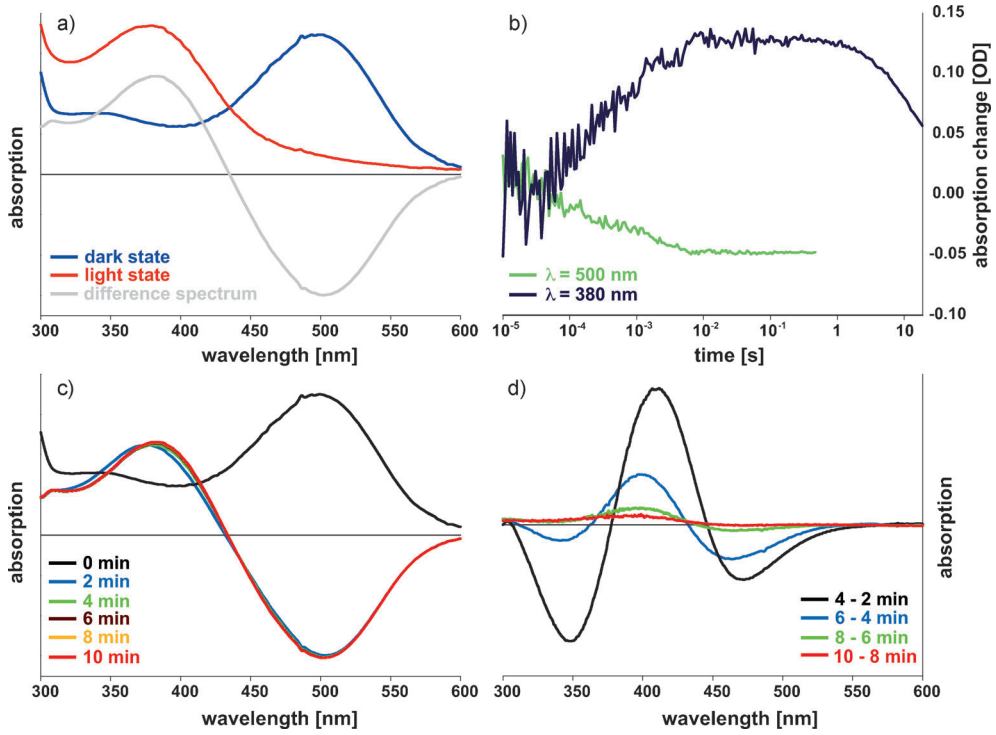

Figure 5. a) Absorption spectra of the rhodopsin dark state (blue) and after continuous illumination (red). The corresponding difference spectrum is depicted in gray. b) Time-resolved absorption changes after photoexcitation with a short laser pulse (5 ns) monitored at 380 nm (blue) and at 500 nm (green). c) Difference spectra between the absorption spectra of rhodopsin after photoexcitation at different time points and the dark state (black). d) Double difference spectra from the spectra shown in (c).

on a timescale of hundreds of microseconds (Figure 5b). The photoproduct itself decays further on a timescale of tens of seconds. Difference spectra and double difference spectra at distinct delay times after laser excitation are depicted in Figure 5c,d. The difference signal decays on a timescale of several minutes. At least three different species cause the spectral changes.[1] The UV-absorbing species meta II rises on a millisecond timescale at 380 nm. The later photointermediate exhibits a bathochromic shift (465 nm) characteristic of meta III. After a few minutes, the meta III state converts into a species where the retinal is released from the Schiff base. The free retinal exhibits an absorption maximum around 380 nm.

The time-resolved NMR experiments reveal that the tryptophan reporter groups were affected differently in the two states, in line with the previous conclusion that motions in rhodopsin are segmental.[18] W126, W161, and W265 show a common half-life of approximately four to five minutes, which corresponds to decay kinetics of the meta II state. The three largest chemical shift perturbations correspond to the tryptophan residues (W126, W161, W265), which show the same first half-life t_1, whereas the two minor chemical shift perturbations correspond to the tryptophan residues (W35 and W175), which do not report on the fast kinetics associated with t_1. Thus, the kinetic data and chemical shift perturbation data are in agreement. Furthermore, W126, W161, and W265 are highly conserved among GPCRs,[19] thereby emphasizing the importance of these residues in the activation process of rhodopsin and GPCRs in general. The second kinetic process observed has a half-live of approximately 24 minutes (t_2). Only W35 and W175 show this half-life.

Kinetic analysis reveals two major processes corresponding to the two time constants t_1 and t_2. We propose that the two time constants t_1 and t_2 represent decay kinetics via the meta II or meta III photocycle alternatives, respectively. The meta II decay (t_1) shows an amplitude of $73 \pm 8\,\%$, while the kinetic process attributed to the meta III decay shows an amplitude of $26 \pm 7\,\%$. These values are highly consistent with ratios of meta II/meta III previously determined by fluorescence spectroscopic studies that support the presence of a meta III state under our conditions used for NMR spectroscopy.[20] The NMR data reveal that the meta II and meta III states emerge in parallel in a relative ratio of approximately 3:1, which was unambiguously confirmed by flash photolysis experiments. In the meta II state, rhodopsin is active and induces the visual signal transduction cascade, while no signal transduction is observed for the meta III state, thus indicating that the structural differences between the two states are directly related to activity.

The kinetic behavior observed for tryptophan residues can be classified into three different types: 1) meta II only, 2) meta II and meta III, and 3) meta III only. One residue, W161, shows only meta II kinetics. W161 is located in the middle of helix 4 and, even though this helix is not involved in the most intense structural rearrangements, it is directly adjacent to helix 3 and is affected by the large rearrangement process involving helix 3 (see Movie S2 at 00:07–00:19, and Figure S6). This influence is indeed observable by the change in the signal intensity of W161 as detected in the 1D ^{15}N-filtered ^{1}H NMR spectra (Figure 4a). In contrast, W126 and W265 show meta II and meta III kinetics. Their involvement in both processes is in agreement with what is seen in flash photolysis experiments, where retinal kinetics can be recorded, and can be rationalized in the context of the rhodopsin structure, because both residues, W126 and W265, are tightly linked to the retinal. For W265, the interaction of its indole ring with the β ionone ring of retinal is disrupted upon rhodopsin activation, visible in the lumirhodopsin intermediate, and the retinal is free to relax and move (see

Movie S2 at times 00:20–00:32, and Figure S6). The rearrangement contributes significantly to the meta II and meta III kinetics observed for W265, since retinal is released from rhodopsin in both intermediates and leads to a significant change in the chemical environment. The structural reorientation of retinal drives the rearrangement of the hydrogen network that connects helix 3 with helix 5 in which W126 is involved (see Movie S2 at times 00:32–00:44, and Figure S6).[21] W126 takes part in this hydrogen-bond network and is thus modulated by the same process. The changes in the signal intensity of W126 are attributed to the significant changes in the hydrogen-bond pattern between residues W126, E122, and H211 (see Movie S2 at times 00:32–00:44, and Figure S6).

Finally, W35 and W175 show exclusively meta III kinetics. The two residues are located in the extracellular domain at the N-terminal end of helix 1 and the E_2-loop, respectively (see Movie S2 at times 00:44–00:56 and at 00:56–01:09, respectively, and Figure S6). The large structural rearrangements known for the meta II state are not observed in the vicinity of W35 and W175. As a consequence of their unique position at hinge regions, both residues are not structurally perturbed during the photocycle, which is consistent with the comparatively small changes in the chemical shift seen upon activation with light (Figure 4a). Despite the spatial distance to the retinal, the decays of their NMR signals display meta III kinetics. Since both tryptophan residues are located close to the E_2-loop of rhodopsin, it is tempting to speculate that the E_2-loop plays a major role in the formation and decay of meta III. The E_2-loop contains β-sheet secondary structural elements that are part of the retinal binding pocket and, importantly, the disulfide bridge connecting the β-sheet to helix 3 that is crucial for stability and folding of rhodopsin.[22] The E_2-loop is also involved in ligand binding in many other GPCRs.[23]

In addition to affording functional insight into the rhodopsin activation process, the experiments presented here also constitute an important advance in method development for the study of membrane protein structure and dynamics in solution: we show that time-resolved liquid-state NMR spectroscopy can be utilized to characterize the kinetics of structural changes of membrane receptors. The technique provides, therefore, a unique opportunity to link information from structural snapshots obtained by X-ray crystallography with spatially resolved kinetic information in solution.

Received: November 4, 2013
Published online: February 6, 2014

Keywords: bovine rhodopsin · G-protein coupled receptors · membrane protein dynamics · NMR spectroscopy · photocycles

[1] O. P. Ernst, F. J. Bartl, *ChemBioChem* **2002**, *3*, 968 – 974.
[2] a) H. Nakamichi, T. Okada, *Angew. Chem.* **2006**, *118*, 4376 – 4379; *Angew. Chem. Int. Ed.* **2006**, *45*, 4270 – 4273; b) S. T. Menon, M. Han, T. P. Sakmar, *Physiol. Rev.* **2001**, *81*, 1659 – 1688; c) K. Palczewski, T. Kumasaka, T. Hori, C. A. Behnke, H. Motoshima, B. A. Fox, I. Le Trong, D. C. Teller, T. Okada, R. E. Stenkamp, M. Yamamoto, M. Miyano, *Science* **2000**, *289*, 739 – 745; d) H. Nakamichi, T. Okada, *Proc. Natl. Acad. Sci. USA* **2006**, *103*, 12729 – 12734; e) H. W. Choe, Y. J. Kim, J. H. Park, T. Morizumi, E. F. Pai, N. Krauss, K. P. Hofmann, P. Scheerer, O. P. Ernst, *Nature* **2011**, *471*, 651 – 655; f) J. H. Park, P. Scheerer, K. P. Hofmann, H. W. Choe, O. P. Ernst, *Nature* **2008**, *454*, 183 – 187; g) C. Altenbach, A. K. Kusnetzow, O. P. Ernst, K. P. Hofmann, W. L. Hubbell, *Proc. Natl. Acad. Sci. USA* **2008**, *105*, 7439 – 7444; h) T. D. Dunham, D. L. Farrens, *J. Biol. Chem.* **1999**, *274*, 1683 – 1690.
[3] S. S. Lefkowitz, D. L. Lefkowitz, J. Kethley, *Am. J. Case Rep.* **2012**, *13*, 66 – 68.
[4] S. J. Hug, J. W. Lewis, C. M. Einterz, T. E. Thorgeirsson, D. S. Kliger, *Biochemistry* **1990**, *29*, 1475 – 1485.
[5] S. Ye, E. Zaitseva, G. Caltabiano, G. F. Schertler, T. P. Sakmar, X. Deupi, R. Vogel, *Nature* **2010**, *464*, 1386 – 1389.
[6] a) F. J. Bartl, R. Vogel, *Phys. Chem. Chem. Phys.* **2007**, *9*, 1648 – 1658; b) R. Vogel, F. Siebert, X. Y. Zhang, G. Fan, M. Sheves, *Biochemistry* **2004**, *43*, 9457 – 9466.
[7] a) D. L. Farrens, H. G. Khorana, *J. Biol. Chem.* **1995**, *270*, 5073 – 5076; b) J. K. McBee, K. Palczewski, W. Baehr, D. R. Pepperberg, *Prog. Retinal Eye Res.* **2001**, *20*, 469 – 529.
[8] A. Mendez, M. E. Burns, A. Roca, J. Lem, L. W. Wu, M. I. Simon, D. A. Baylor, J. Chen, *Neuron* **2000**, *28*, 153 – 164.
[9] E. Ritter, M. Elgeti, F. J. Bartl, *Photochem. Photobiol.* **2008**, *84*, 911 – 920.
[10] T. Okada, M. Sugihara, A. N. Bondar, M. Elstner, P. Entel, V. Buss, *J. Mol. Biol.* **2004**, *342*, 571 – 583.
[11] J. Standfuss, P. C. Edwards, A. D'Antona, M. Fransen, G. Xie, D. D. Oprian, G. F. X. Schertler, *Nature* **2011**, *471*, 656 – 660.
[12] M. Kumauchi, T. Ebrey, *Handbook of Photosensory Receptors* (Eds: W. R. Briggs, J. L. Spudich), Wiley-VCH, Weinheim, **2005**, p. 43 – 76.
[13] a) J. Klein-Seetharaman, E. V. Getmanova, M. C. Loewen, P. J. Reeves, H. G. Khorana, *Proc. Natl. Acad. Sci. USA* **1999**, *96*, 13744 – 13749; b) M. C. Loewen, J. Klein-Seetharaman, E. V. Getmanova, P. J. Reeves, H. Schwalbe, H. G. Khorana, *Proc. Natl. Acad. Sci. USA* **2001**, *98*, 4888 – 4892; c) J. Klein-Seetharaman, P. J. Reeves, M. C. Loewen, E. V. Getmanova, J. Chung, H. Schwalbe, P. E. Wright, H. G. Khorana, *Proc. Natl. Acad. Sci. USA* **2002**, *99*, 3452 – 3457.
[14] a) E. Getmanova, A. B. Patel, J. Klein-Seetharaman, M. C. Loewen, P. J. Reeves, N. Friedman, M. Sheves, S. O. Smith, H. G. Khorana, *Biochemistry* **2004**, *43*, 1126 – 1133; b) K. Werner, C. Richter, J. Klein-Seetharaman, H. Schwalbe, *J. Biomol. NMR* **2008**, *40*, 49 – 53.
[15] K. Werner, I. Lehner, H. K. Dhiman, C. Richter, C. Glaubitz, H. Schwalbe, J. Klein-Seetharaman, H. G. Khorana, *J. Biomol. NMR* **2007**, *37*, 303 – 312.
[16] T. Kühn, H. Schwalbe, *J. Am. Chem. Soc.* **2000**, *122*, 6169 – 6174.
[17] a) S. Kaushal, K. D. Ridge, H. G. Khorana, *Proc. Natl. Acad. Sci. USA* **1994**, *91*, 4024 – 4028; b) S. S. Karnik, H. G. Khorana, *J. Biol. Chem.* **1990**, *265*, 17520 – 17524; c) B. E. Olausson, A. Grossfield, M. C. Pitman, M. F. Brown, S. E. Feller, A. Vogel, *J. Am. Chem. Soc.* **2012**, *134*, 4324 – 4331.
[18] T. E. Woudenberg-Vrenken, A. L. Lameris, P. Weissgerber, J. Olausson, V. Flockerzi, R. J. Bindels, M. Freichel, J. G. Hoenderop, *Am. J. Physiol.* **2012**, *303*, G879 – 885.
[19] A. B. Patel, E. Crocker, P. J. Reeves, E. V. Getmanova, M. Eilers, H. G. Khorana, S. O. Smith, *J. Mol. Biol.* **2005**, *347*, 803 – 812.
[20] M. Heck, S. A. Schadel, D. Maretzki, K. P. Hofmann, *Vision Res.* **2003**, *43*, 3003 – 3010.
[21] a) M. Beck, T. P. Sakmar, F. Siebert, *Biochemistry* **1998**, *37*, 7630 – 7639; b) E. Zaitseva, M. F. Brown, R. Vogel, *J. Am. Chem. Soc.* **2010**, *132*, 4815 – 4821.
[22] A. J. Rader, G. Anderson, B. Isin, H. G. Khorana, I. Bahar, J. Klein-Seetharaman, *Proc. Natl. Acad. Sci. USA* **2004**, 101, 7246 – 7251.

[23] a) A. Straßer, H.-J. Wittmann, R. Seifert, *J. Pharmacol. Exp. Ther.* **2008**, *326*, 783 – 791; b) M. Scarselli, B. Li, S.-K. Kim, J. Wess, *J. Biol. Chem.* **2007**, *282*, 7385 – 7396; c) J. M. M. Laurila, H. Xhaard, J. O. Ruuskanen, M. J. M. Rantanen, H. K. Karlsson, M. S. Johnson, M. Scheinin, *Br. J. Pharmacol.* **2007**, *151*, 1293 – 1304; d) H. Preuss, P. Ghorai, A. Kraus, S. Dove, A. Buschauer, R. Seifert, *Naunyn-Schmiedeberg's Arch. Pharmacol.* **2007**, *376*, 253 – 264.

[24] a) A. Knowles, A. Priestley, *Vision Res.* **1978**, *18*, 115 – 116; b) see Ref. [13b]; c) D. D. Oprian, R. S. Molday, R. J. Kaufman, H. G. Khorana, *Proc. Natl. Acad. Sci. USA* **1987**, *84*, 8874 – 8878; d) P. J. Reeves, N. Callewaert, R. Contreras, H. G. Khorana, *Proc. Natl. Acad. Sci. USA* **2002**, *99*, 13419 – 13424; e) P. J. Reeves, J. M. Kim, H. G. Khorana, *Proc. Natl. Acad. Sci. USA* **2002**, *99*, 13413 – 13418; f) P. Schanda, E. Kupce, B. Brutscher, *J. Biomol. NMR* **2005**, *33*, 199 – 211.

